A q-state clock-like phase transition in a coupled XY model

Chia-Chi Shih[1,*], Ching-Hsing Pei[2], Kai-Huang Chen[3], Chien-Min Cheng[2]

[1] General Education Center, TungFang Design Institute, Kaohsiung City, Taiwan
[2]Department of Electronic Engineering, Southern Taiwan University of Science and Technology, Tainan City, Taiwan
[3] Department of Electronics and Information Engineering, TungFang Design Institute, Kaohsiung City
shih560506@gmail.com

Abstract: This study adopts the Monte Carlo simulation method to investigate a coupled XY model on two-dimensional triangular lattices. The simulation reveals a q-state clock-like phase transition in addition to the original XY phase transition. Analyzing the spin histograms exposes that the strong on-site coupling tends to lock the difference between the phase variables of the two XY order parameters and generates an additional phase transition. The novel discrete q-state symmetry arising from the coupling term is demonstrated to joint the continuous symmetry of the model in this investigation.
[Chia-Chi Shih, Ching-Hsing Pei, Kai-Huang Chen, Chien-Min Cheng. **A q-state clock-like phase transition in a coupled XY model.** *Life Sci J* 2013;10(3):298-302] (ISSN:1097-8135). http://www.lifesciencesite.com. 47

Keywords: KT transition, coupled XY model, q-state clock model

1. Introduction

There has much research interest in statistical models that simultaneously display both continuous and discrete symmetries. Kosterlitz and Thouless[1] have explained that the two-dimensional XY phase transition is not a conventional continuous phase transition, but rather involves the breakage of bound pairs of the topological vortex and antivortex in the system. Although the continuous aspect of phase transition in XY model has been studied extensively, the Mermin-Wagner[2] theorem does not exclude the possibility of discrete symmetry breaking. We propose a coupled XY model to investigate the competition between the continuous and discrete phase transitions. Physical systems that simultaneously display both discrete and continuous symmetries have received considerable interest. Three-state Potts-like phase transitions involving herringbone order have been investigated. The XY continuous transition might compete with some discrete transitions in the system. The Ising-like phase transition was taken into account in competing with Kosterlitz-Thouless transition in He^3 superfluid film.[3] Thus Lee et al. examined the nonuniversal critical behavior in a coupled XY-Ising model.[4] Notably, the classical XY model can be expressed as many forms of coupled XY model and with variation of the temperature or other parameters, two or more successive transitions can occur in the case of strongly coupled excitation. Jiang et al.[5,6] studied a coupled XY model based on a Hamiltonian proposed by Bruinsma and Aeppli[7] for smectic liquid crystals. The on-site coupling between the two XY ordering parameters in the proposed model can generate discrete phase transitions, such as Potts transitions[8]. Jiang et al.[9] demonstrated a unique three-state Potts-like discrete transition following the continuous XY transition in the system. Jiang et al. also found two different orderings established simultaneously via a single continuous phase transition in some coupling parameter domain. Moreover, they used the new phenomena to interpret the liquid crystal Sm-A to Hex-B transition.[10,11] Considerable interest exists in the competition between the continuous phase transition and the discrete aspect in two-dimensional XY systems and in smectic liquid crystal layers.[12,13] A coupled XY model is proposed in this investigation, in which a possible q-fold disturbance similar to that three-fold one of Jiang et al. is introduced to the on-site coupling. The proposed model reveals versatile properties and several distinct phase transitions occur. Besides the classical XY transition, a unique q-state clock transition is generated in the intrinsic XY system.

2. Physical model and analysis

The coupled XY Hamiltonian in this investigation is as follows

$$H = -J_1 \sum_{<i,j>} \cos(\theta_i - \theta_j) - J_2 \sum_{<i,j>} \cos(\varphi_i - \varphi_j) - J_3 \sum_{i} \cos(\theta_i - q\varphi_i)$$

where the first and the second terms are XY models themselves and the coupling term is introduced in the third term. Two angular variables θ_i and φ_i are located at each triangular lattice site i. For the experimental importance, it is more realistic to simulate the model on the triangular lattice than the square lattice. <i,j> represents the nearest-neighbor pairs of sites and denotes the nearest-neighbors'

coupling in the first two terms. The third term shows that the coupling between the two XY order parameters is localized at the same lattice site. The integer number q of coupled XY model will decide coupling form of the two order parameters. It is noted that as the θ and φ are coupled relatively strongly, the phase transitions are quite interesting. Therefore J_3 = 3.1 (larger than both J_1 and J_2) is chosen to examine the phenomena in the following studies.

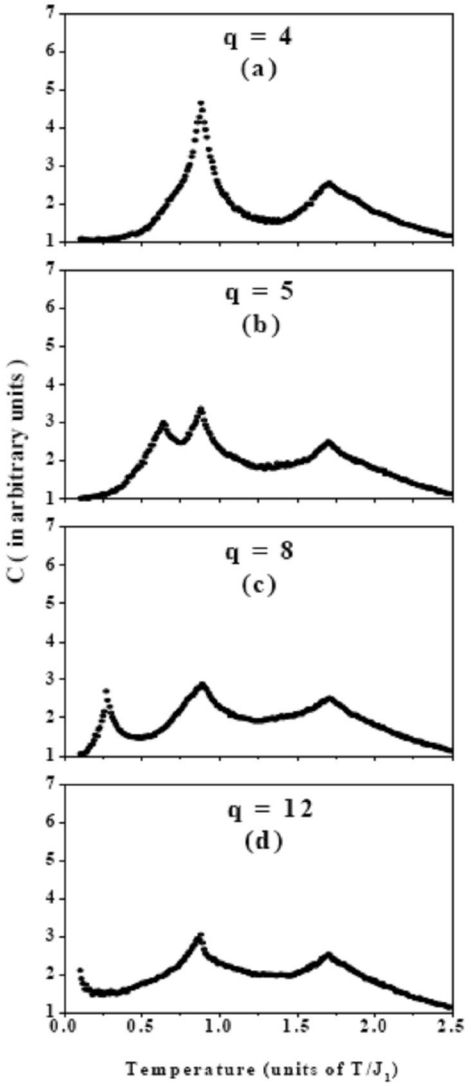

Fig.1.Heat-capacity (C) versus temperature. Figures (a), (b), (c) and (d) display the cases of q= 4, 5, 8 and 12, respectively.

The simple scenario, the case of $J_1 > J_2$ (say, J_1 = 1.0 and J_2 = 0.5), is explored in this investigation. Employing the standard Monte Carlo technique, we conducted the simulation works on 36X36 triangular lattices with periodic boundaries. The heat-capacity data as a function of temperature for various q were obtained by calculating the energy fluctuation $C_V = \frac{1}{NT^2}(< H^2 > - < H >^2)$, as displayed in Figs. 1(a) – 1(d). During the simulation, the angles θ_i and φ_i are treated as continuous unconstrained variables. 1,000,000 Monte Carlo steps (MCS) are used for each temperature. To ensure thermal equilibrium, the first 200,000 MCS are discarded. There appear two heat-capacity peaks for $q \leq 4$, and three peaks for $q > 4$. This phenomenon shows that the system proceeds through two phase transitions for $q \leq 4$, and pass through three phase transitions for $q > 4$. We show the heat-capacity diagram of the case q = 4 in Figs. 1(a), a sharp peak is located at T = 0.88 and a broad hump appears around T = 1.7. (The temperature is in unit of J_1 in this study.). The heat-capacity diagrams of q = 5, q = 8, and q = 12 are displayed in Figs. 1(b), 1(c), and 1(d), respectively. All of the figures display a broad hump around T = 1.7. In the case of q = 4, another sharp peak shows at T = 0.88. It is noted that for the cases of $q > 4$, the sharp peak at the lower temperature is divided into two peaks. An extra transition appears and these two peaks constitute a critical transition region. The new peak of the transition further shifts to the lower temperature as the value q increases. For the case of q = 5, the peak is located at T = 0.64. For the case of q = 8, the peak is located at T = 0.27. For q=12, the temperature of the lowest heat-capacity peak approaches zero, as shown in the figure. Comparing with the smooth heat capacity peak of KT type transition these heat capacities peaks are rather singular. They are affected by the strong coupling of the two order parameters. Especially in the case of q = 3, the two peaks would combined to transition simultaneously. And the transition belongs to the special university class in discussing the exponents of the heat capacity and the helicity modulus.

To illustrate the nature of these phase transitions, the spin histograms of the states near the heat-capacity peaks for various values of q are analyzed directly. For the case of q = 4, Figs. 2(a) and 2(e) illustrate histograms of parameters θ_i and φ_i at low temperature T = 0.1, we find both θ_i and φ_i are accumulative and exhibit a single hump. Raising the temperature to T = 0.7, which is below the first phase transition (whereas T_{C1} = 0.88). The distributions of both θ_i and φ_i still exhibit a single hump as shown in Figs. 2(b) and 2(f). Notably, φ_i initiates small satellite peaks. The temperature is raised gradually to T = 1.0, which is the temperature between the first and second phase transition, T_{C2} = 1.7. Figures 2(c) and 2(g) display the spin distributions of θ_i and φ_i. Despite the distribution of θ_i still displaying a single hump, the distribution of φ_i separates into four distinct peaks with almost equal height in one period 2π of φ_i with equal interval of $2\pi/4$. Further increasing the

temperature to above the T_{C2}, the spin distributions at T = 1.8 are drawn in Figs. 2(d) and 2(h). Both spin distributions of θ_i and φ_i were observed to smear out and distribute over all angles equally. Such that orders θ and φ both display an isotropic character.

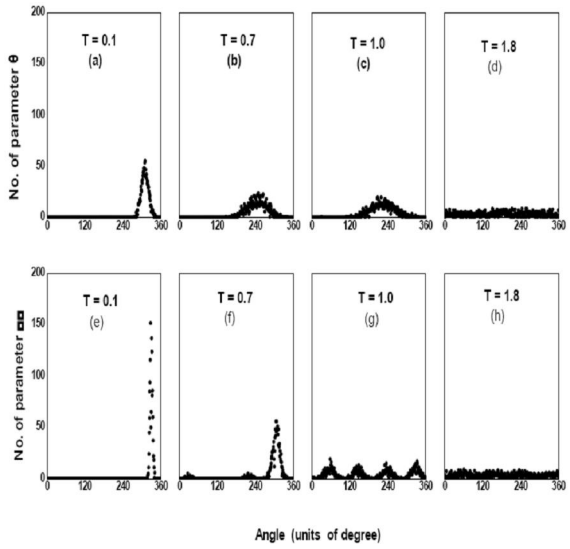

Fig. 2. Histograms for parameters θ_i and φ_i of the case q = 4.

For the case of q = 5, the unusual histograms of φ_i near the heat-capacity peaks are illustrated in Figs. 3(a)-3(d). The distribution of θ_i is not shown here because it has the similar evolution to that of the former case of q = 4 for various values of q. At low temperature T = 0.1, the distribution of φ_i displays a single peak as shown in Fig. 3(a). At T = 0.7, which is the temperature between the first and second transition temperature (T_{C1} = 0.64, T_{C2} = 0.88) in the critical region, three peaks rather than the original concentrated single peak are shown in Fig. 3(b). Notably, the number of peaks of the distribution of φ_i increases with increasing temperature. Further increasing the temperature to just above the T_{C2}, the distribution of φ_i separates into five distinct peaks with almost equal height in one period 2π of φ_i with equal interval of $2\pi/5$. The spin distribution of φ_i at T = 1.0 is shown in Fig. 3(c). Figure 3(d) displays the spin distributions of φ_i at T = 1.8, which is the temperature just above the third phase transition (T_{C3} = 1.7). The spin distribution of φ_i is smeared out and spread over all angles equally. For the case of q = 8, the distribution evolution of φ_i is similar to the case of q = 5 as shown in Figs. 3(e) – 3(h). For the case of q = 12, at T = 0.1, the spin distribution of φ_i appears three peaks as shown in Fig. 3(i). The first transition temperature is supposed to be lower than T = 0.1. The distribution evolution of φ_i near the other transition temperature is similar to the cases of $q \geqq 5$. As shown in the Fig. 3(j), the distribution of φ_i reveals nine peaks at T = 0.7, which is below T_{C2} (T_{C2} = 0.88). And at T = 1.0, Fig. 3(k) shows that the distribution of φ_i separates into twelve distinct peaks with almost equal height in one period 2π of φ_i with equal interval of $2\pi/12$. At T = 1.8, higher than T_{C3} (T_{C3} = 1.7), the φ_i order distributes over all orientation as shown in Fig. 3(l).

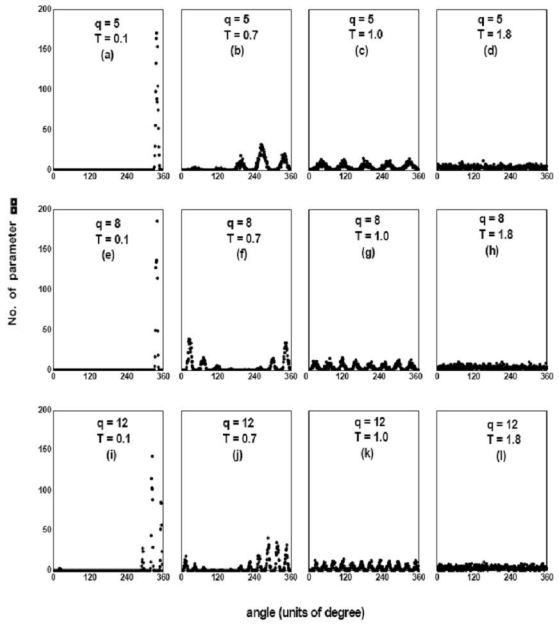

Fig. 3. Histograms of the parameter φ_i.

The spin histograms at T = 0.1, 0.7, 1.0 and 1.8 show that orders θ and φ proceed through several distinct phase transitions. At low temperatures (T < 0.1), both θ and φ are ordered, and both spin distributions are accumulative. The bond orientational order corresponds to $\theta_i \approx \theta_j$ and $\varphi_i \approx \varphi_j$. Notably, $\theta_i \approx \varphi_i$ also, owing to the strong on-site coupling of J_3. At temperatures higher than T_{C1}, θ order remains unchanged, φ order starts the first XY-like phase transition into multi-fold degenerate state. The coupling resulting from the third term will be unable to guide the orientation of φ to follow that of θ. Thus, the bond orientation of order parameter φ evolves into multiple directions corresponding to the equivalent energy minima in this temperature range. For $q \leq 4$, the system passes through the transition into a steady q folder degenerate state. For q > 4, the system goes through the transition into multi-fold degenerate intermediate state, and more degeneracy

occurs as the temperature is increasing. As the temperature is raised to $T > T_{C2}$, the on-site J_3 coupling generates q equivalent steady energy minima in one period 2π of φ_i with equal interval of $2\pi/q$. The bond orientation of φ divides into q distinct directions, and the order parameter of φ proceeds through the second phase transition. The system exhibits q disorder freedom for the φ parameter in the degenerate energy state. The simulation results are also inspected by use of the energy histograms and the Binder's fourth-order cumulant of energy.[14] The analysis does not reveal any signal of the first order phase transition. A q-state clock model presented one second-order transition for $q \leq 4$, two KT transitions for $q > 4$. As the parameter q increases the lower transition temperature approaches zero, leaving one KT transition in the system. The simulation results present characters of discrete symmetry resemble that of the q-state clock model. As the temperature is further raised, the system melts and proceeds through the last XY phase transition. Both θ and φ then are melted into a completely disordered phase. The simulation reveals the unique q-state clock-like phase transition in addition to the original XY phase transitions. Analyzing the spin histograms exposes that the strong on-site coupling tends to lock the difference between the phase variables between the two XY order parameters and thus generates an additional phase transition.

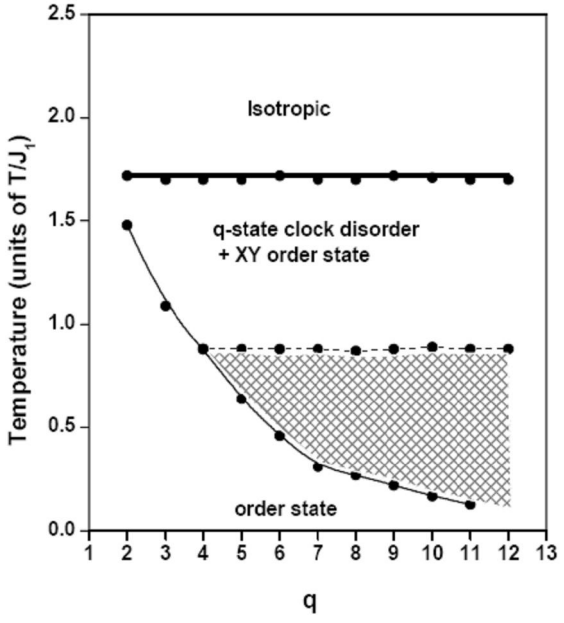

Fig. 4. Phase diagram of transition temperature versus state parameter q.

In order to illustrate the occurrence of the q-state clock-like phase transition, we summarize the simulation data to plot the phase diagram. Figure 4 shows the schematic diagram of phase transition sequences as the function of parameter q. The solid dots are determined by the peaks of heat-capacity. The heavy line at T = 1.7 denotes the XY isotropic transition in the system. For $q > 4$, the q-state intermediate transition at T = 0.88 is denoted by the dash line. The thin line presents the lowest transition temperature. As the parameter q increases, the transition shifts to lower temperatures. The q-state clock intermediate phase is located in the grid region between the dash line and the light line. It is assumed that as the coupling strength is lowered down and the parameter q is sufficient large, the discrete q-state clock-like transition of the coupled XY model would evolve back to the original continuous XY transition.

3. Discussion and Conclusions

To summarize the results, we examine a unique coupled XY model on in two-dimensional triangular lattices by use of the Monte Carlo simulation. The phase transition in the model reveals both continuous and discrete symmetries. The system proceeds through two phase transitions for $q \leq 4$, through three phase transitions for $q > 4$. Analyzing the spin histograms of θ_i and φ_i shows that the φ order precedes the discrete q-state clock-like phase transition. As the value q is sufficient large, the discrete q-state clock-like transition would become a continuous XY transition. The occurring of the unique q-state clock-like phase transition in addition to the XY phase transition is due to the coupling term, which tends to lock the difference between the phase variables of the two XY systems. The coupled XY model ascertains that a discrete symmetry arising from the coupling term joints to the original continuous symmetries. And the competition of continuous and discrete symmetries is also demonstrated in the investigation.

Corresponding Author:
Chia-Chi Shih, Ph.D.
General Education Center,
Tung Fang Design Institute,
Kaohsiung City, Taiwan
E-mail: shih560506@gmail.com

References

1. J. M. Kosterlitz and D. J. Thouless, J. Phys. C 6 1973; 1181.
2. N. D. Mermin and H. Wagner, Phys. Rev. Lett. 1966; 22;1133.
3. D. L. Stein, and M. C. Cross, Phys. Rev. Lett. 1979;42;504.
4. D. H. Lee, J. D. Joannopoulos, J. W. Negele, and D. P. Landau, Phys. Rev. B 1986;33;450.
5. I. M. Jiang, T. Stoebe and C. C. Huang, Phys. Rev. Lett. 1996;76;2910.
6. C. C. Shih, and I. M. Jiang, Physica A 2005;385; 366.
7. R. Bruinsma and G. Aeppli, Phys. Rev. Lett. 1982;48;1625.
8. F. Y. Wu, Rev. Mod. Phys. 1982;54;235.
9. I. M. Jiang and C. C. Huang, Physica A 1995;221; 104.
10. T. Stoebe, C. C. Huang, and J. W. Goodby, Phys. Rev. Lett. 1992;68; 2944.
11. T. Stoebe, I. M. Jiang, S. N. Huang, A. J. Jin and C. C. Huang, Physica A 1994;205; 108.
12. D. R. Nelson, and B. I. Halperin, Phys. Rev. B 1980;21; 5312.
13. C. Dasgupta, Int. J. of Mod. Phys. B 1995;9; 2219.
14. K. Binder, and D. W. Heermann, Monte Carlo Simulation in Statistical Physics, Springer, Berlin, 1988.

07/12/2013